Short-period volcanic gas precursors to phreatic eruptions: Insights from Poás Volcano, Costa Rica

9 authors, including:

Alessandro Aiuppa
Università degli Studi di Palermo
347 PUBLICATIONS   7,410 CITATIONS

SEE PROFILE

Javier Pacheco
National University of Costa Rica
37 PUBLICATIONS   1,895 CITATIONS

SEE PROFILE

Geoffroy Avard
National University of Costa Rica
64 PUBLICATIONS   545 CITATIONS

SEE PROFILE

Marco Liuzzo
National Institute of Geophysics and Volcanology
88 PUBLICATIONS   1,658 CITATIONS

SEE PROFILE

Some of the authors of this publication are also working on these related projects:

Project   ICE-VOLC: multiparametrIC Experiment at antarctica VOLCanoes: data from volcano and cryosphere-ocean-atmosphere dynamics (PNRA: Programma Nazionale di Ricerche in Antartide) View project

Project   Quantification of the depletion of ozone in the plume of Mount Etna View project

Short-period volcanic gas precursors to phreatic eruptions: Insights from Poás Volcano, Costa Rica

J.M. de Moor [a,b,c,*], A. Aiuppa [c,d], J. Pacheco [a], G. Avard [a], C. Kern [e], M. Liuzzo [d], M. Martínez [a], G. Giudice [d], T.P. Fischer [b]

[a] Observatorio Vulcanológico y Sismológico de Costa Rica, Universidad Nacional, Heredia, Costa Rica
[b] Department of Earth and Planetary Sciences, University of New Mexico, Albuquerque, NM, USA
[c] Dipartimento DiSTeM, Università di Palermo, Palermo, Italy
[d] Istituto Nazionale di Geofisica e Vulcanologia, Sezione di Palermo, Italy
[e] USGS Volcano Disaster Assistance Program, Cascades Volcano Observatory, Vancouver, WA, USA

A B S T R A C T

Volcanic eruptions involving interaction with water are amongst the most violent and unpredictable geologic phenomena on Earth. Phreatic eruptions are exceptionally difficult to forecast by traditional geophysical techniques. Here we report on short-term precursory variations in gas emissions related to phreatic blasts at Poás volcano, Costa Rica, as measured with an in situ multiple gas analyzer that was deployed at the edge of the erupting lake. Gas emitted from this hyper-acid crater lake approaches magmatic values of SO_2/CO_2 1–6 days prior to eruption. The SO_2 flux derived from magmatic degassing through the lake is measureable by differential optical absorption spectrometry (sporadic campaign measurements), which allows us to constrain lake gas output and input for the major gas species during eruptive and non-eruptive periods. We can further calculate power supply to the hydrothermal system using volatile mass balance and thermodynamics, which indicates that the magmatic heat flux into the shallow hydrothermal system increases from $\sim$27 MW during quiescence to $\sim$59 MW during periods of phreatic events. These transient pulses of gas and heat from the deeper magmatic system generate both phreatic eruptions and the observed short-term changes in gas composition, because at high gas flux scrubbing of sulfur by the hydrothermal system is both kinetically and thermodynamically inhibited whereas CO_2 gas is always essentially inert in hyperacid conditions. Thus, the SO_2/CO_2 of lake emissions approaches magmatic values as gas and power supply to the sub-limnic hydrothermal system increase, vaporizing fluids and priming the hydrothermal system for eruption. Our results suggest that high-frequency real-time gas monitoring could provide useful short-term eruptive precursors at volcanoes prone to phreatic explosions.

© 2016 The Authors. Published by Elsevier B.V. This is an open access article under the CC BY license (http://creativecommons.org/licenses/by/4.0/).

1. Introduction

Volcanic eruptions involving explosive vaporization of meteoric water are common occurrences on our wet planet. Of the $\sim$18,000 volcanic eruptions listed in the Global Volcanism Database since 1900, 822 ($\sim$5%) are considered phreatic in nature (Global Volcanism Program, 2013). Eruptions that occur through surface water account for $\sim$8% of historic eruptions but have claimed a disproportionate number of human lives ($\sim$20% of total deaths) (Mastin and Witter, 2000). The diverse hazards related to wet eruptions

contribute to their deadliness, and include base surges, ballistics, lahars, tsunamis, and toxic gases. Lahars generated by explosive ejection of crater lake water are the most dangerous hazard associated with volcanic lakes and have killed >16,000 people in historical times (Mastin and Witter, 2000).

Phreatic eruptions are exceptionally challenging to forecast because many do not directly involve the movement of magma, which generates distinct geophysical signals useful in eruption forecasting, and may occur simply due to subtle changes in shallow hydrothermal systems (Rouwet et al., 2014a). Documented precursors of phreatic activity show long to medium term changes in geophysical (i.e. seismicity, deformation, and gravimetry) or geochemical (i.e. lake water and gas compositions) parameters (Barberi et al., 1992; Rouwet et al., 2014b; Sano et al., 2015), but accurate short-term (days) eruption forecasting remains excep-
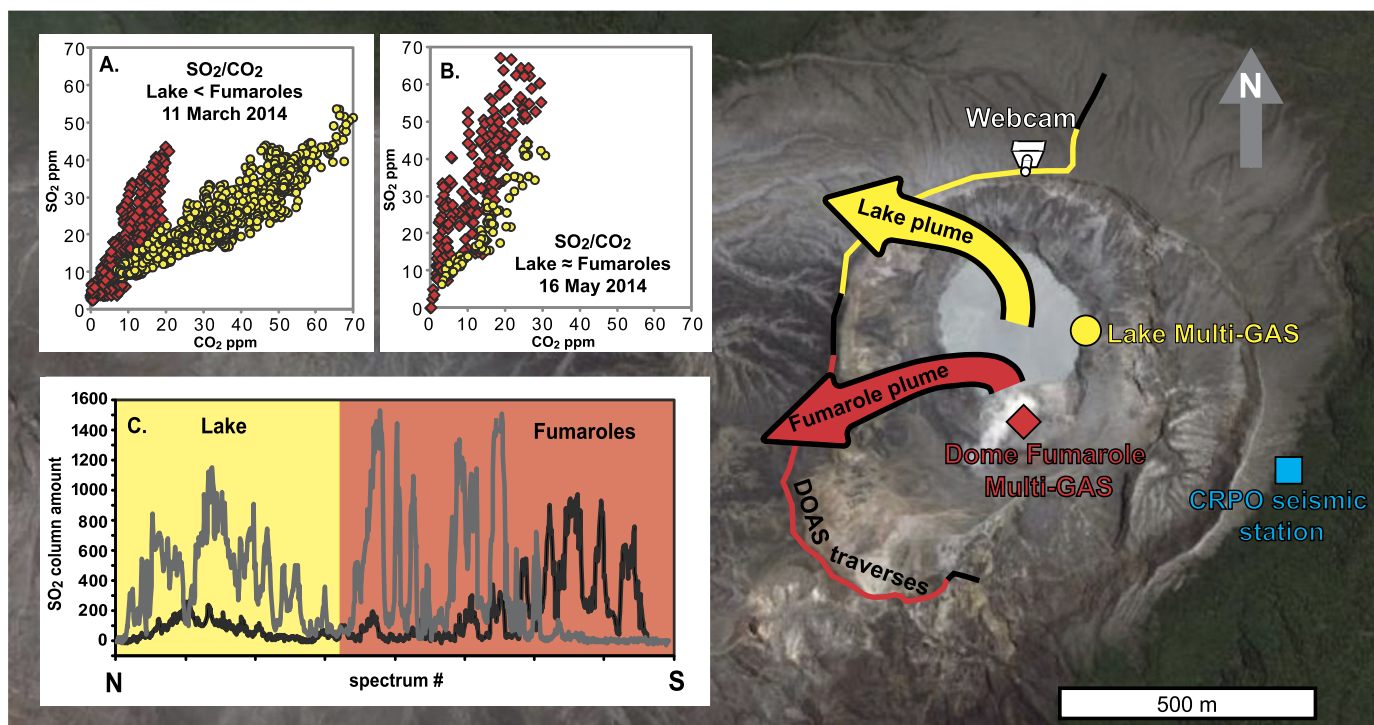
Fig. 1. The Poás crater and general characteristics of gas emissions. Multi-GAS measurement sites (Lake and Dome Fumaroles), the CRPO seismic station, the webcam, and DOAS traverse path are indicated. Webcam images show that the fumarolic plume rises buoyantly and travels to the SW for >95% of the time (Supplementary Materials; Fig. S6; Movie S2). The gas plume from the lake is diffuse and transparent, and rises buoyantly to the NW (Movie S2). Inserts A and B show example Multi-GAS datasets collected on 11 March 2014 during a period of low eruptive activity and on 16 May 2014 during a period of intense phreatic activity, respectively. The fumarolic (red diamonds) and lake gas (yellow circles) compositions are clearly distinguishable on 11 March, but similar on 16 May. Insert C shows example DOAS traverses (column amounts in ppm.m) in which lake and fumarole gas plumes are distinguished. The traverse in gray was conducted on 30 September 2014, 5 days before a climax in phreatic eruptions, and shows a strong SO_2 plume from the lake. The traverse in black was conducted on October 16, after the climax and at the beginning of a period with no eruptions and shows a much weaker lake SO_2 plume. Background image from Google Earth. (For interpretation of the references to color in this figure legend, the reader is referred to the web version of this article.)

tionally challenging. For example, at some well-monitored volcanoes with crater lakes, precursory seismicity has been observed to occur just minutes before phreatic eruptions (Jolly et al., 2010; Kaneshima et al., 1996) or is entirely absent (Christenson et al., 2007).

Published cases of precursory changes in gas geochemistry prior to phreatic eruptions are rare. This is probably because most attention from the scientific community has focused on volcanoes prone to large magmatic eruptions. However, the 27 September 2014 eruption at Ontake-San Volcano (Japan) claimed 57 victims (with 6 still missing), highlighting the need for more focused research on this relatively poorly studied class of volcanic activity and the wet volcanoes where frequent phreatic activity can dominate restless behavior, without apparent movement or eruption of magma. Recently, Sano et al. (2015) reported a decadal-scale change in He isotope compositions towards more magmatic values at Ontake prior to the fatal phreatic blast. White Island in New Zealand is a well-monitored volcano with an ephemeral crater lake, high temperature fumaroles, and is prone to phreatic eruptions. Werner et al. (2008) recognized large changes in bulk plume gas chemistry over a period of years (2002–2006) after the formation of a crater lake in 2003. Both SO_2 flux and SO_2/CO_2 approached magmatic values and were accompanied by a increase in seismic activity; however no eruptions directly followed the escalation. Ruapehu is another well-monitored volcano in New Zealand that hosts an active crater lake. Airborne gas monitoring revealed that SO_2 flux and SO_2/CO_2 both increased in the year to months prior to the 25 September 2007 phreatomagmatic eruption (Christenson et al., 2010). Nevado del Ruiz volcano in Columbia also had a highly active crater lake before the 1985 Plinian eruption. Giggenbach et al. (1990) considered this eruption to be between magmatic and

phreatic in character, because the blast ejected only older magmatic rocks (Williams et al., 1986) and was driven by magmatic gas pressure buildup below a sealed carapace produced by the sublimnic hydrothermal system. The expulsion of lake water and melting of summit ice due to this "pneamato-magmatic" (Giggenbach et al., 1990) eruption generated an acidic lahar that killed >20,000 people from the town of Armero. In contrast to the cases at White Island (Werner et al., 2008) and Ruapehu (Christenson et al., 2010), where gases became more magmatic with increasing activity, gas compositions at Nevado del Ruiz became more hydrothermal in composition a few months before the eruption (Giggenbach et al., 1990). These studies suggest that decadal to monthly scale precursory changes in gas compositions likely occur at many volcanoes prone to phreatic (and related) eruptions. However, the cause of the changes and the specific conditions triggering sudden and potentially deadly phreatic explosions not associated with magmatic movement are poorly understood. The recognition of associated short-term changes in gas chemistry is essentially absent for these complex magmatic-hydrothermal systems and their eruptions, but could be essential in forecasting individual explosive blasts.

Our study focuses on Poás volcano (N 10.1968°; W 84.2305°) in Costa Rica, which entered a period of phreatic activity in 2006. The eruptive period culminated in a series of relatively large phreatic blasts (columns >300 m) between June and October of 2014, after which the volcano entered a period of repose that continues until present time. Poás volcano hosts a warm acidic lake (Laguna Caliente; $T \sim 50\,°C$, pH ~ 0 at the time of study) of about 270 m diameter, as well as high-temperature (up to $\sim 800\,°C$) fumaroles adjacent to the lake (Dome Fumaroles; Fig. 1). The Poás crater represents one of the most chemically extreme environments on Earth and Poás Volcano National Park was visited by >200,000
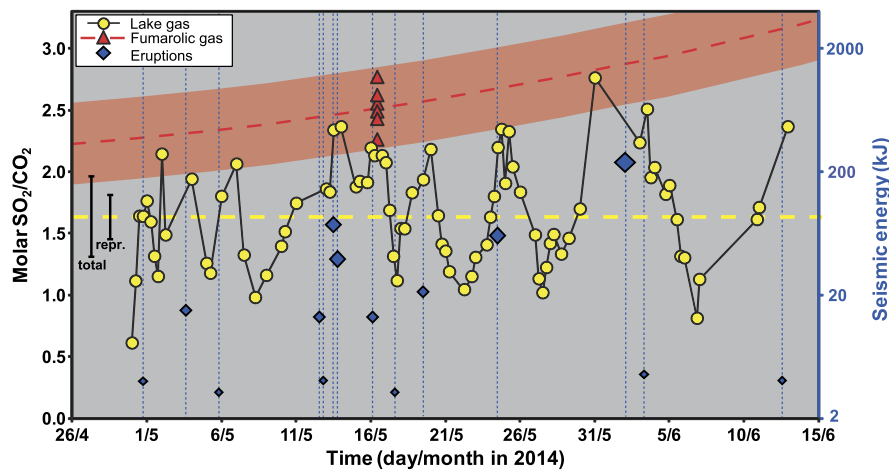
Fig. 2. Time series of lake gas SO_2/CO_2 and seismic energy (SE) of eruptions. The yellow dashed line is the median of lake gas SO_2/CO_2 (1.64). Total error in Multi-GAS measurements is conservatively estimated at 20% from experimental results (± 0.33 for SO_2/CO_2 of 1.64; see Methods), whereas the average reproducibility of the lake gas measurements is 0.18 (error bars shown at left). The composition of the dome fumaroles was measured on 16 May, and the fumarolic compositional trend is constrained by Multi-GAS campaigns between January and July of 2014 (Fig. S3). The sizes of the blue diamonds correspond to phreatic eruption groups as defined by SE (Fig. 3). (For interpretation of the references to color in this figure legend, the reader is referred to the web version of this article.)

tourists in 2014. About 60 seismically registered phreatic blasts occurred from the lake during the same year, ranging from minor "gas bursts" to highly explosive jets ejecting ballistics, sediments, vapor and lake water to >400 m above the lake surface (Movie S1). Poás explosions are a type example of phreatic eruptions through a crater lake, displaying a vertical jet of solids and fluids accompanied by a radial base surge of vapor (Fig. S1, Movie S1), and no juvenile magmatic material is erupted. Short-term geophysical precursors heralding an imminent eruption are absent. Long-term (2001 to 2014) and sporadic fumarole gas chemistry monitoring recently showed how the dynamics of the volcano-hydrothermal system are reflected in changes in gas discharges (Fischer et al., 2015). Here we focus on the short-term (days to weeks) variations in plume gas compositions that provide new insights on the processes that lead to phreatic eruptions.

2. Materials and methods

2.1. Field methods

We conducted an experiment to assess high-frequency temporal variations in lake gas composition at Poás from April to June 2014, which was a period of intense phreatic activity. A fully autonomous Multi-Component Gas Analyzer System (Multi-GAS) (Aiuppa et al., 2007) was installed at the shore of the lake (Fig. 1). The fixed "lake" Multi-GAS instrument records concentrations of CO_2, SO_2, H_2S, and H_2O at a rate of 0.1 Hz. The instrument is programmed to acquire data for 30 min four times a day, which allowed us to derive a time-series of gas ratios (Fig. 2, Table S1) that are independent of mixing with air. Gas ratios are determined by linear regression through gas concentration data (Aiuppa et al., 2013), as shown in Fig. S2. The site of the lake Multi-GAS station was carefully chosen to target pure lake gas emissions, and was located in a sheltered cove on the upwind side of the lake, where lake gas emissions tend to form a local eddy below a ~10 m cliff (see Supplementary Text). Data gaps in the time series are due to conditions in which not enough gas reached the station for robust determination of SO_2/CO_2 (i.e. SO_2 concentrations <5 ppm) or where a programmed analysis session failed due to lack of charge on the battery (i.e. persistent low light conditions, or solar panel damaged by 2 June eruption). The near-real time data from this fixed lake station (Fig. 2; Table S1) were supplemented with occasional campaign measurements conducted with a portable Multi-GAS to char-

acterize the chemical composition of the dome fumaroles (Fig. 1; Fig. S3).

Fourteen seismically registered eruptions occurred during the 44 days of data acquisition by the lake Multi-GAS station. The largest phreatic eruption of 2014 occurred on June 2, ejecting ballistics and sediments to >400 m height, which destroyed peripheral components of the lake station. The station continued to record data until June 12, at which point the battery was drained. During campaign measurements, fumarole temperature was measured with infrared camera from the eastern lake shore, and walking traverses with ultraviolet spectrometers for Differential Optical Absorption Spectroscopy (DOAS) determination of SO_2 emission rate (Galle et al., 2002) were conducted along the western crater rim (Fig. 1). The lake plume is distinguishable from the fumarolic plume by DOAS under typical weather conditions (Fig. 1 inset C).

2.2. Uncertainties in Multi-GAS measurements

Errors in Multi-GAS measurements of gas ratios are paramount in determining whether the time series trends in SO_2/CO_2 (Fig. 2) are confidently resolved. As we are also comparing data collected with two different instruments (fixed unit for lake gases, mobile unit for fumarole gases), it is also necessary to take into account errors associated with each instrument. The overall uncertainty (combined accuracy and precision) in SO_2/CO_2 for the type of Multi-GAS instruments was reported to be $\leq 20\%$ by Aiuppa et al. (2009). Based on laboratory experiments, Pering et al. (2014) reported the Multi-GAS error in SO_2/CO_2 to be $\leq 15\%$.

We assess analytical errors associated with Multi-GAS measurements in two ways. First, we conducted a series of experiments using gas mixtures of known SO_2/CO_2 to assess the total error (accuracy and reproducibility) of both of our Multi-GAS stations (see Supplementary Text, Figs. S4 and S5, Tables S2 and S3). The gas mixtures have a range in composition similar to those observed at Poás, from 2.54 to 0.16, and the experiments were conducted in ambient outdoor conditions in Heredia, Costa Rica, to mimic field conditions. These results confirm that total error is better than 20% (at 95% confidence level) for SO_2/CO_2 for both instruments (Supplementary Text, Figs. S4 and S5, Tables S2 and S3).

Of fundamental importance to this study is whether the trends in SO_2/CO_2 shown in Fig. 2 are resolved with confidence. In this regard, instrumental precision or reproducibility is most important. Thus, the second assessment of errors was conducted using

the acquired time series field data by calculating multiple SO_2/CO_2 values for each 30 minute data acquisition period to quantify reproducibility (Table S1). Each analysis includes subtraction of background CO_2 signal (i.e. from air), and optimization of the R^2 of linear regression, typically using >30 individual gas CO_2 and SO_2 concentration data points. SO_2/CO_2 values were calculated by multiple linear regression determinations on subsets of data within each half hour analytical session, allowing quantification of reproducibility for many of the individual datapoints shown in Fig. 2. This approach indicates that the average SO_2/CO_2 reproducibility is 0.18 (or 11% of the median observed SO_2/CO_2 value; See Supplementary Text for further details). The measured variations in SO_2/CO_2 are far greater than the 20% error margin or the precision/reproducibility as determined by multiple linear regression assessments within datasets. We also note that the 20% analytical errors margins are greater than the precision values in the vast majority (86%) of cases, suggesting that the gases measured by the lake Multi-GAS station are homogeneous on very short timescales (i.e. within the 30 min analysis interval).

2.3. Intercontamination of gas sources

Changes in environmental conditions can also affect the robustness of Multi-GAS measurements. For our purposes, the most important effect to consider is that of wind direction and the possibility of intercontamination between lake and fumarolic gas (Shinohara et al., 2015). The measurements of fumarolic gas composition were conducted manually and in close proximity to the source, allowing the operator to accurately target gas originating from the fumaroles. Mobile Multi-GAS measurements of the fumarolic gas are conducted on top of the dome to the south of the lake (Fig. 1, Movies S1 and S2) and the high gas concentration and poor visibility (a full face gas mask required) in the fumarolic plume make it exceedingly obvious to the operator when true fumarolic gas is being measured.

In the field it is also visually obvious that the fumarolic gas plume does not usually travel close to the site of Lake Multi-GAS station, however it is less trivial to quantitatively prove that our fixed Multi-GAS station lake gas compositions are not affected by mixing with fumarolic gas. We can however track the fumarolic plume direction using webcam footage, as is shown in Fig. S6 and Movie S1. The wind direction at Poás is almost always towards the west and based on assessment of all of the available webcam footage recorded during the deployment of the lake Multi-GAS instrument, we find that the fumarolic plume traveled towards the west or southwest (away from the Multi-GAS station) for 97.6% of the time. The plume traveled towards the camera (north) for 1.7% of the time, and east (towards the Multi-GAS) for 0.7% of the time. When the fumarolic plume does travel towards the east, it is when there is very little wind and the plume rises buoyantly above the Lake Multi-GAS station. In none of the webcam footage have we observed a time period during a Multi-GAS analysis (i.e. the 2 h per 24 h that the instrument was actually acquiring data) where the fumarolic plume was traveling towards the lake Multi-GAS station.

Our second test for fumarole gas contamination is based on the difference in H_2S/SO_2 between the fumarolic and lake gas compositions. No H_2S was detected in the lake emissions during mobile Multi-GAS measurements or by the fixed lake station during the period of study, whereas the fumarolic gas contained H_2S well above the detection limit of the Multi-GAS. This distinction between fumarolic and ultra-acidic lake gas emissions has also been observed at Aso volcano, Japan (Shinohara et al., 2015), and at Copahue volcano, Argentina (Tamburello et al., 2015). However, the H_2S detection limit for Multi-GAS instruments is not trivial to determine precisely, and is dependent on the cross sensitivity of the

H_2S electrochemical sensor to SO_2 gas. We determined the cross sensitivity during Multi-GAS calibrations by introducing H_2S-free gas with known SO_2 concentration to the instrument and measuring the apparent concentration of H_2S. For both of our instruments, the cross sensitivity of the H_2S sensor to SO_2 is $20 \pm 2\%$, thus at 50 ppm SO_2 (roughly the highest concentrations observed in the Lake Multi-GAS emission data), the apparent H_2S concentration is 10 ± 1 ppm. After correction for SO_2 cross sensitivity (H_2S concentration = H_2S apparent concentration – $20 \pm 2\% \times SO_2$ concentration), we observe no discernable H_2S, with an estimated detection limit of 1 ppm.

Based on SO_2 concentrations in lake Multi-GAS measurements and the H_2S/SO_2 values measured in the fumarolic gas plume (average of 0.12) at Poás, we can assess the expected H_2S concentrations if the gas measured by the lake Multi-GAS station originating from the fumaroles. This analysis shows that for 21 lake Multi-GAS measurements where high SO_2 concentrations and high SO_2/CO_2 values are observed, H_2S concentrations up to 5.9 ppm would be expected if the measured gas were fumarolic. The maximum H_2S concentrations observed in the lake Multi-GAS data are ≤ 1 ppm, which is below the detection limit. Therefore, we find no compositional evidence that the high observed SO_2/CO_2 values measured in the lake gas emissions are due to fumarolic gas from the dome traveling to the fixed Lake Multi-GAS site.

3. Results

The results of the lake Multi-GAS experiment show that significant short-period changes occur in lake gas emission composition. These variations are correlated with eruptive activity. Fig. 2 shows the SO_2/CO_2 (molar) as a function of time in Poás crater lake emissions as measured by the lake Multi-GAS station between April and June 2014 (Table S1). Even considering our conservative estimations of error, the time series trends in SO_2/CO_2 measured by the lake Multi-GAS are statistically significant (Spearman's rho tests on monotonic data segments indicate r values >0.9) and the variations are well beyond reasonable estimations of total error. Phreatic eruptions are plotted with their associated radiated seismic energy (SE, in units of kJ), which is used throughout as a relative measure of eruptive magnitude only (Table S4; see Supplementary Information). Our dataset, the first high-frequency time series of gas compositions acquired during phreatic eruptions, demonstrates that explosions occur after measurable short-term increases in SO_2/CO_2. Importantly, the composition of lake gas emissions approaches but does not surpass the SO_2/CO_2 value of the high temperature fumaroles and all of the largest eruptions (SE > 30) are preceded by trends of increasing SO_2/CO_2 starting two to six days beforehand. Our values of SO_2/CO_2 for the fumaroles are similar to the ratios measured in the highest temperature direct gas samples from Poás (Rowe et al., 1992) and are consistent with regional trends in SO_2/CO_2 (Aiuppa et al., 2014).

In order to statistically characterize the relationship between eruptions and lake gas composition, we initially consider the proportion of eruptions associated with SO_2/CO_2 values above the median SO_2/CO_2 value (1.64) of the lake Multi-GAS dataset to those associated with SO_2/CO_2 below the median. Considering the SO_2/CO_2 measurement closest in time to the occurrence of each eruption (Table S5), all but one of the fourteen eruptions have $SO_2/CO_2 \geq 1.64$. If we define the SO_2/CO_2 of each eruption as the mean value of gas compositions recorded within 12 h of the eruption time, thirteen of the fourteen eruptions have $SO_2/CO_2 > 1.64$, and for a 24 h time window, eleven eruptions have associated $SO_2/CO_2 > 1.64$ (Fig. 3). Thus, phreatic eruptions are at least 3 times more likely to be associated with high SO_2/CO_2 than not within a meaningful time window for monitoring purposes. The discordant phreatic events are of low energy, with SE < 10 (Fig. 3,
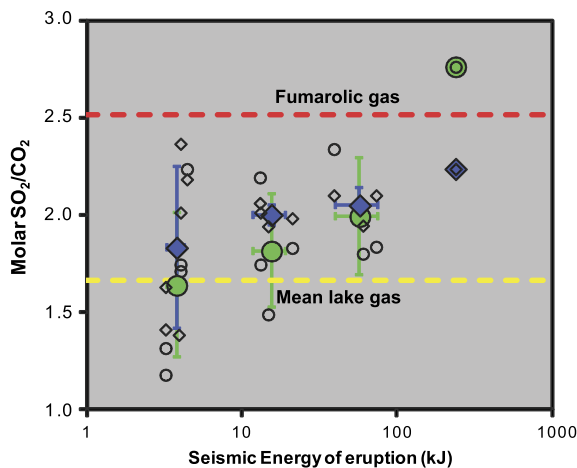
Fig. 3. Relationship between SO_2/CO_2 and SE. Diamonds are the average SO_2/CO_2 recorded within 24 h of eruption and circles indicate the closest SO_2/CO_2 value measured before each eruption. The individual eruptions (open symbols) naturally fall into four categories (closed symbols) based on seismic energy: SE < 10; 10 < SE < 30; 30 < SE < 150; SE > 150. Small eruptions on average are associated with lower SO_2/CO_2 and display high variance, whereas large eruptions show high associated SO_2/CO_2, closest to fumarolic gas. This relationship is maintained considering only precursory gas measurements (green filled circles) and the generally lower SO_2/CO_2 values observed before eruptions reflect the fact that eruptions tend to occur before the peak in SO_2/CO_2 (Fig. 2). (For interpretation of the references to color in this figure legend, the reader is referred to the web version of this article.)

values; Fig. 4), 26 are associated with a phreatic blast with SE > 10 within 36 h (true positive values) and 14 are not (false positive values). The ratio of true positives to total number of positives gives a statistical measure of the association between high SO_2/CO_2 and eruption, which is 0.65 for eruptions of SE > 10 and a time window of 36 h. This ratio is known as "true predicted value", and increases with the number of eruptions considered and larger time window (Fig. 4). Importantly, the ratio of true negatives (low SO_2/CO_2 and no eruption) to total number of negatives (Fig. 4; no eruption "predicted" based on low SO_2/CO_2) is high for the most dangerous eruptions, and approaches 1 for eruptions with SE > 30 and short time window (Table S5). The results show that both true predicted values (successful "prediction" of eruption based on high SO_2/CO_2) and false predicted values (successful "prediction" of quiescence based on low SO_2/CO_2) are high, indicating strong evidential worth for the association between gas composition and eruptions.

It is important to note that "predictive" in the sense of the above statistical analysis demonstrates trait associations between gas composition and the occurrence of eruptions, but does not prove that changes in SO_2/CO_2 occur before eruptions in a predictive sense useful for eruption forecasting. However, the transition from low to high SO_2/CO_2 prior to eruption occurs gradually over a period of days (Fig. 2), providing the possibility of developing a practically viable short-term precursory indicator of imminent eruption. We envisage a hypothetical tool for forecasting phreatic eruptions in which the slope of the SO_2/CO_2 trend (Fig. 2, Fig. 5) is evaluated in real time considering lake Multi-GAS data collected during a defined time window (Fig. 5). The choice of time window depends firstly on a practical factor, which is data completeness and existence of data gaps due to low gas concentration (i.e. unfavorable meteorological conditions) or technical issues (usually low battery charge). The second consideration is timely response of the slope parameter to changes in gas composition. Choice of a shorter time window results in more variable slope values, more periods where the slope cannot be calculated due to too few data, but more rapid response of the parameter to changes in gas composition. Choice of a longer time window results in smoother but slower response, with fewer periods where the slope cannot be calculated (Fig. 5). For our dataset, 48 h and 90 h seem to be useful time windows to consider, with the shorter time window capturing changes in gas composition rapidly enough to show changes in slope sign prior to some eruptions that are not captured by the longer time window (e.g. 19 May eruption, Fig. 5). However, the shorter time window also produces a noisier response of the slope parameter that can cause false negative scenarios (e.g. gap and negative slope on 12–13 May during a series of eruptions; Fig. 5).

Table S5), which do not pose a serious risk even to scientists working in the crater. The eruptions naturally fall into four groups based on SE (Fig. 3). Those with SE < 10 display high variability in terms of associated SO_2/CO_2, whereas all of those with SE > 10 have associated SO_2/CO_2 > 1.9 and their SO_2/CO_2 ratio displays a positive correlation with SE (diamonds in Fig. 3). If we consider the SO_2/CO_2 recorded prior to each eruption (Table S5; circles in Fig. 3) all but one eruption with SE > 10 show a precursory SO_2/CO_2 value greater than the median value (1.64) and the positive relationship between SO_2/CO_2 and SE is preserved.

We further explore the association between gas composition and the occurrence and energy of phreatic blasts by categorizing each lake gas data point based on diagnostic statistical tests to determine whether an eruption occurred within a given time window of the measurement (Fig. 4). In this analysis we follow the method of Biggs et al. (2014), considering time windows of 24 h, 36 h, and 48 h, and the occurrence of eruptions with SE > 1 (i.e. all seismically registered eruptions), SE > 10 (8 eruptions), and SE > 30 (combining the 4 largest eruptions into one group; Fig. 3). Of the 40 measured gas compositions with SO_2/CO_2 > 1.64 (positive

	Eruption	No eruption
SO_2/CO_2 > 1.64	26 True positive	14 False positive
SO_2/CO_2 < 1.64	9 False negative	31 True negative

$\dfrac{\text{# True positives}}{\text{Total # positives}} = 0.65$

$\dfrac{\text{# True negatives}}{\text{Total # negatives}} = 0.78$

| | Eruption Seismic Energy Threshold | | |
	SE > 30	SE > 10	SE > 1
24hr window	0.28	0.53	0.70
36hr window	0.35	**0.65**	0.83
48hr window	0.45	0.78	0.95
24hr window	0.95	0.95	0.70
36hr window	0.93	**0.78**	0.63
48hr window	0.90	0.63	0.48

Fig. 4. Example of diagnostic test for categorizing lake gas SO_2/CO_2 data points and association with eruption (left). A true positive result is if an eruption of SE > X (10 in this case) occurs within Y h (36 h here) of a measured gas composition with SO_2/CO_2 > Z (1.64; the mean lake gas composition in this case). A false positive is if no eruption of SE > X occurs within Y h of a gas measurement with SO_2/CO_2 > Z. A true negative result is if no eruption of SE > X occurs within Y h of a gas measurement with SO_2/CO_2 < Z. A false negative result is if an eruption of SE > X occurs within Y h of a gas measurement with SO_2/CO_2 < Z. This last category (eruptions associated with low SO_2/CO_2) is the least desirable scenario for hazards assessment. Eruptions with SE < 10 present little danger even to scientists working within the crater. The table on the right shows ratios of true positive results to total positive results and true negative results to total negative results (i.e. positive predicted values and negative predicted values; top and bottom, respectively) considering different SE thresholds (see Figs. 2 and 3) and time windows. For more complete results and errors see Table 1 and Table S6.

Table 1

Excerpt of diagnostic test results on the statistical relationship between SO_2/CO_2 and the occurrence of phreatic eruptions within a given time window of the measurement (see Table S6 for full results). The number of cases is given for true positives, false positives, false negatives and true negatives for a SO_2/CO_2 gas ratio threshold of 1.64. The number of cases where the measured SO_2/CO_2 value falls within analytical error of the defined gas ratio threshold is given for each set of conditions. See text and Fig. 4 for details.

	Eruption threshold					
	SE > 30 (n = 4)	Within error	SE > 10 (n = 8)	Within error	SE > 1 (n = 14)	Within error
12 h window						
True positives	8	4	13	4	20	6
False positives	32	8	27	8	20	6
False negatives	1	1	1	1	5	2
True negatives	39	9	39	9	35	8
True positives/total positives	0.20		0.33		0.50	
True negatives/total negatives	0.98		0.98		0.88	
24 h window						
True positives	11	4	21	5	28	7
False positives	29	8	19	7	12	5
False negatives	2	1	2	1	12	4
True negatives	38	9	38	9	28	6
True positives/total positives	0.28		0.53		0.70	
True negatives/total negatives	0.95		0.95		0.70	
36 h window						
True positives	14	4	26	7	33	8
False positives	26	8	14	5	7	4
False negatives	3	1	9	3	15	5
True negatives	37	9	31	7	25	5
True positives/total positives	0.35		0.65		0.83	
True negative/total negatives	0.93		0.78		0.63	
48 h window						
True positives	18	5	31	9	38	11
False positives	22	7	9	3	2	1
False negatives	4	1	15	3	21	6
True negatives	36	9	25	7	19	4
True positives/total positives	0.45		0.78		0.95	
True negatives/total negatives	0.90		0.63		0.48	

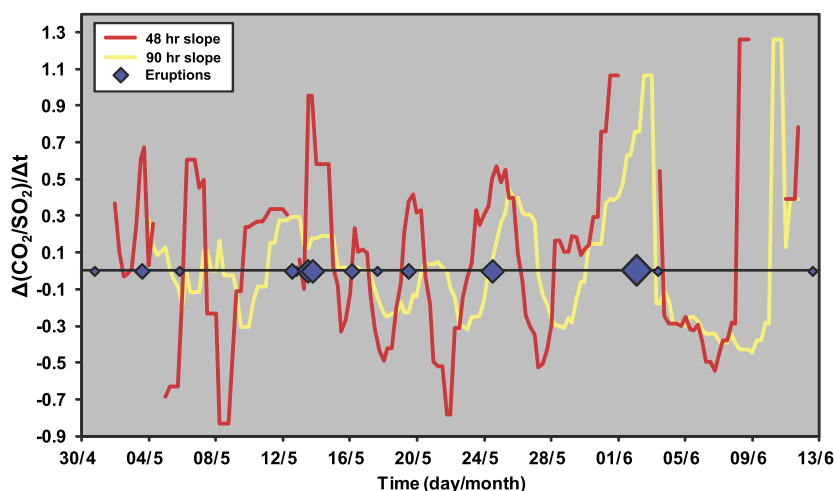**Fig. 5.** Results of slope analysis method for envisioned forecasting of phreatic eruptions based on gas composition time series (Fig. 2). $\Delta(SO_2/CO_2)/\Delta t$ is calculated considering data collected in the past X h in a hypothetical scenario considering data arriving in real time. The size of the blue diamonds indicates eruptions by size as in Fig. 2. Five of the eight eruptions with SE > 10 and three of the four eruptions with SE > 30 are predictable based on the 48 h slope. See Table S7 for summary of results. (For interpretation of the references to color in this figure legend, the reader is referred to the web version of this article.)

The slope analysis uses the data recorded prior to the last recorded data point and thus simulates the hypothetical situation of data arriving in real time, using the most recent data to assess the potential for eruption. The analysis using 48 h and 90 h time windows suggests that based on our actual data it would be possible to accurately forecast five out of the eight phreatic eruptions with SE > 10 (Table S7), demonstrating the high potential of real-time gas measurements to improve short-term forecasting of phreatic eruptions at volcanic lakes. The slope parameter is also successful at forecasting periods of quiescence. Negative slope values are associated with lack of eruptive events, and the ratio of true negative scenarios to total negatives (as assessed for Fig. 4 and Table 1) is greater than 0.8 for eruptions with SE > 10 for both 48 and 90 h time windows (Table S7).

The relationship between gas composition and eruptions also holds for the medium term at Poás, as no eruptions have occurred since October 2014 and campaign Multi-GAS measurements show the SO_2/CO_2 of lake gas emissions were consistently <0.5 in 2015

and at the beginning of 2016. More importantly perhaps, our data show statistically significant relationships between gas compositions and the occurrence of phreatic eruptions (Fig. 4) that yield a conceptual model for the short-term mechanisms that generate phreatic eruptions, which may be more widely applicable to monitoring wet volcanoes.

4. Discussion

The variations in SO_2/CO_2 in emissions from the Poás crater lake can be understood in terms of the relative susceptibility of SO_2 and CO_2 to reaction with hydrothermal fluids. The crater lake is the surface expression of an extensive hydrothermal system, contains a layer of liquid native sulfur at its base (Bennett and Raccichini, 1978; Oppenheimer and Stevenson, 1989), is rich in dissolved sulfate, and precipitates a diverse array of sulfur bearing minerals from its waters (Delmelle et al., 2000; Martínez et al., 2000). These secondary sulfur phases are derived from hydrolysis of magmatic gases injected into the sub-limnic hydrothermal system (Martínez et al., 2000). The dominant reaction in stripping SO_2 from magmatic gases in the crater lake is (Delmelle et al., 2000; Kusakabe et al., 2000):

$$3SO_{2(g,aq)} + 2H_2O_{(l)} = S^o_{(s,l)} + 2HSO^-_{4(aq)} + 2H^+_{(aq)} \qquad (1)$$

as evidenced by sulfate-rich lake waters (Martínez et al., 2000) and abundant floating sulfur spherules (Movie S2). The degree of S isotope fractionation between HSO^-_4 and elemental S ($\Delta^{34}S_{HSO^-_4-S^o}$ + 23.3‰) in the lake strongly supports the dominance of equation (1) (Kusakabe et al., 2000; Rowe, 1994). Sulfur isotope fractionation between native sulfur and bisulfate, and oxygen isotope fractionation between water and bisulfate indicate chemical and isotopic equilibration temperatures (>250 °C) far in excess of measured lake temperatures (∼50 °C). High SO_2/CO_2 and high SO_2/H_2S in crater lake emissions also indicate gas equilibration temperatures (∼300 °C) far higher than lake temperatures (Tamburello et al., 2015). Therefore, the dynamics of the higher temperature sublimnic hydrothermal system are primarily responsible for the dominant compositional features of the gas emitted from the lake. Thermodynamics of reaction 1 dictate that SO_2 gas is less reactive at higher temperature and lower pH. Significantly, no H_2S was observed in crater lake gas emissions during the period of this study (above the Multi-GAS detection limit of ∼1 ppm in SO_2-rich gas; see section 2.3), whereas the H_2S/SO_2 measured in the fumaroles was 0.07–0.26. Importantly, H_2S injected into the sublimnic hydrothermal system is therefore completely stripped from gas entering the lake by partitioning into liquid native S, precipitation of sulfides, and reaction with SO_2 to form polythionates and elemental S (Delmelle et al., 2000). Disproportionation reactions producing H_2S from SO_2, commonly thought to be the "smoking gun" for gas interaction with hydrothermal fluids (Symonds et al., 2001), are not significant in the Poás lake, calling for re-examination of gas–water interaction processes (Tamburello et al., 2015). Whereas S is partially stripped from the magmatic gas input to the lake, CO_2 is effectively inert in acidic fluids and efficiently passes through the hydrothermal-lake system (Christenson et al., 2010).

We suggest that the short-term variations in SO_2/CO_2 in the lake gas emissions are due to varying influx of magmatic gas, which also determines whether phreatic eruptions occur or not. Comparing all DOAS lake SO_2 flux measurements (19 traverses conducted between March and November 2014 in which the lake and fumarolic plumes are distinguishable; Fig. 1, Table 2), the mean SO_2 flux associated with periods of phreatic activity is 81.4± 23.9 T/day ($n = 11$), whereas during non-eruptive episodes the lake SO_2 flux is 26.5±8.9 T/day ($n = 8$). Increased gas flux reduces gas residence time and the interaction between gas species and
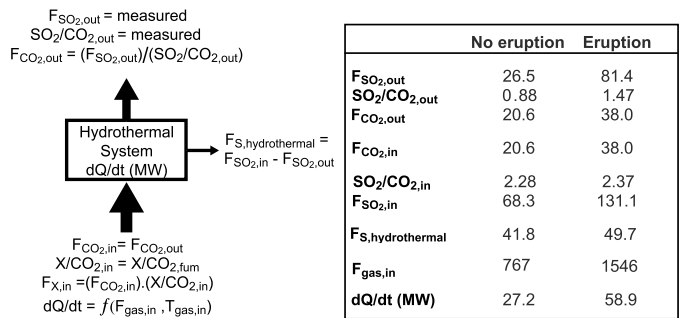

	No eruption	Eruption
$F_{SO_2,out}$	26.5	81.4
$SO_2/CO_{2,out}$	0.88	1.47
$F_{CO_2,out}$	20.6	38.0
$F_{CO_2,in}$	20.6	38.0
$SO_2/CO_{2,in}$	2.28	2.37
$F_{SO_2,in}$	68.3	131.1
$F_{S,hydrothermal}$	41.8	49.7
$F_{gas,in}$	767	1546
dQ/dt (MW)	27.2	58.9

Fig. 6. Box model for gas inputs and outputs for the Poás hydrothermal system (see Table 2). The SO_2 flux from the system ($F_{SO_2,out}$; all fluxes in units of T/day) and $SO_2/CO_{2,out}$ are constrained by DOAS and Multi-GAS measurements, respectively, allowing calculation of the CO_2 flux from the lake ($F_{CO_2,out}$). The CO_2 flux from the lake is equal to the CO_2 flux into the lake ($F_{CO_2,in}$) because CO_2 is inert in acidic fluids. The composition of gas feeding the lake is constrained by gas ratios measured at the high temperature fumaroles ($X/CO_{2,fum}$; where $X = H_2O, SO_2, H_2S$, and H_2), which allows calculation of the flux of gases into the crater lake ($F_{X,in}$) and the flux of S lost to the hydrothermal system ($F_{S, hydrothermal}$; expressed in T/d SO_2). As the flux and composition of magmatic gas into the lake are constrained, the heat transfer to the crater lake (dQ/dt) can be quantified (see supplementary online text for calculation details).

lake water, kinetically inhibiting SO_2 hydrolysis (Symonds et al., 2001; Tamburello et al., 2015; Werner et al., 2008). Increased input of magmatic volatiles rich in SO_2, HCl, and HF (Fischer et al., 2015; Rowe et al., 1992), also increases the acidity and temperature of sub-limnic (Kusakabe et al., 2000) hydrothermal fluids, both of which shift equation (1) to the left and decrease the efficacy of the hydrothermal system in removing SO_2 from gas (Tamburello et al., 2015). Fig. 6 presents a box model for the Poás lake system allowing calculation of the gas and heat flux into the base of the hydrothermal system (see supplementary online text and Table 2) and the mass of S lost from the gas input during eruptive and non-eruptive periods.

The DOAS results show that during eruptive episodes the SO_2 flux from the lake is ∼3.1 times higher than during non-eruptive episodes, whereas the CO_2 flux is only a factor of ∼1.8 higher. The mass of S lost from the gas to the hydrothermal system is similar during high and low gas flux, indicating that equation (1) has a reduced capacity for removing S from the magmatic gases during times of high volatile input. Thus, kinetics of S hydrolysis, the thermodynamics of the SO_2 disproportionation reaction occurring in the sub-limnic hydrothermal system, and the causative relationship between the injection of hot magmatic gas and phreatic explosions conspire to make SO_2/CO_2 in crater lake gas emissions a sensitive monitoring parameter for detecting short-term gas and heat flux variations leading to phreatic eruptions.

Magmatic gas is the principal source of volatiles (S, Cl, F) in volcanic lakes and also the main source of heat input (Pasternack and Varekamp, 1997), which drives phreatic eruptions. As we can constrain the flux of gas to the lake (Fig. 6) for eruptive and non-eruptive episodes, we can calculate the heat flux for both cases. The heat flux to the lake is determined by integrating the temperature dependent heat capacity functions for H_2O, SO_2, CO_2, H_2, and H_2S from measured fumarolic temperature to the condensation temperature of water (100 °C), and summing the total enthalpy from gas cooling with the enthalpy of evaporation of water (Pasternack and Varekamp, 1997) (see Supplementary Materials and Table 2). The average heat flux calculated for eruptive episodes is 58.9 MW compared to 27.2 MW for non-eruptive episodes (Fig. 5). Based on our seismic record of phreatic eruptions (Table S8) and the correlation between seismicity and column height (Fig. S7) as observed by webcam for a subset of eruptions (27 of the 60 seismically registered eruptions in 2014 were recorded by webcam; Movie S1), we can estimate the col-

Table 2
Flux calculations for Poás cráter lake for non-eruptive and eruptive periods.

Date (dd-mm)		Non-eruptive fluxes					Eruptive fluxes				
		29-04	16-10	29-10	26-11	Non-eruptive Av.	19-03 Av.	16-05	28-08	30-09	Eruptive Av.
Lake output											
SO_2 flux	T/day	18.1	29.6	10.4	47.8	**26.5**	51.6	76.6	94.1	103.4	**81.4**
	±	3.4	10.4	7.4	14.4	**8.9**	11.6	38.3	18.8	26.7	**23.9**
	n	1	4	1	2	**8**	2	1	2	6	**11**
SO_2/CO_2	molar	0.61	0.95	1.08	0.89	**0.88**	0.88	2.07	1.64	1.31	**1.47**
	±	0.04	0.16	0.06	0.21	**0.12**	0.05	0.10	0.50	0.20	**0.21**
CO_2 flux	T/day	20.3	22.1	6.6	39.2	**20.6**	40.4	26.0	42.4	55.3	**38.0**
	±	5.8	13.1	6.9	22.7	**11.6**	13.7	19.0	24.0	24.0	**20.3**
Fumarole gas											
H_2O/CO_2	molar	140.43	91.63	91.63	33.74	**89.36**	130.89	125.25	59.28	80.92	**99.08**
SO_2/CO_2	molar	2.33	2.65	2.65	1.46	**2.28**	2.17	2.44	2.88	2.00	**2.37**
H_2/CO_2	molar	0.36	0.32	0.32	na[*]	**0.33**	na	0.38	na	0.45	**0.41**
H_2S/CO_2	molar	0.21	0.70	0.70	0.17	**0.44**	0.17	0.25	0.32	0.18	**0.23**
H_2O	mol%	97.29	95.15	95.15	92.77	**95.1**	97.51	96.85	93.39	95.71	**95.9**
SO_2	mol%	1.62	2.76	2.76	4.02	**2.8**	1.62	1.89	4.53	2.37	**2.6**
CO_2	mol%	0.69	1.04	1.04	2.75	**1.4**	0.75	0.77	1.58	1.18	**1.1**
H_2	mol%	0.25	0.33	0.33	na	**0.3**	na	0.29	na	0.53	**0.4**
H_2S	mol%	0.15	0.73	0.73	0.46	**0.5**	0.12	0.19	0.50	0.21	**0.3**
FLIR Temp	°C	383	616	405	334	**434.5**	591	337	644	640	**553.0**
Total Q	MJ/kg	2.97	3.41	3.01	2.86	**3.1**	3.38	2.89	3.45	3.46	**3.3**
Lake input											
H_2O flux	T/day	1039	736	221	481	**670**	1923	1186	914	1627	**1369**
SO_2 flux	T/day	69.0	85.3	25.6	83.5	**68.3**	127.8	92.4	177.5	160.9	**131.1**
H_2 flux	T/day	0.7	0.6	0.2	na	**0.6**	n	0.9	na	2.2	**1.4**
H_2S flux	T/day	3.5	12.6	3.8	5.4	**7.5**	5.5	5.4	11.0	8.1	**7.1**
Total gas flux	kg/s	13.1	9.9	3.0	7.0	**8.9**	24.3	15.2	13.2	21.4	**17.9**
Heat flux	MW	39.0	33.8	8.9	20.2	**27.2**	81.9	43.8	45.7	74.2	**58.9**

[*] na = not available.

umn height, as well as the energy released for all events following Brown et al. (1989). The total eruptive power output for 2014 is estimated to be ∼2.5 MW (Table S8). The difference in heat flux to the lake between eruptive and non-eruptive periods is about an order of magnitude higher than the eruptive power, indicating that more than enough energy is available through pulses of increased volatile input from the deeper magmatic system to generate eruptions (Fig. 5). It is worth noting that the amount of energy released during short-lived phreatic eruptions is very high, with instantaneous power of >200 GW for the largest eruptions, implying that energy is stored and catastrophically released below a low permeability seal (Christenson et al., 2007; Fischer et al., 2015; Kaneshima et al., 1996; Sano et al., 2015). Many of the eruptions occur slightly before the peak in SO_2/CO_2 (Fig. 2), perhaps suggesting that during increasing gas flux, an upward propagating front between vapor and liquid dominated hydrothermal regimes (Rowe et al., 1992) encounters a confining zone (a sealed hydrothermal carapace; Christenson et al., 2007, 2010; Giggenbach et al., 1990) saturated in lake water that infiltrated during quiescent episodes. This water is vaporized and pressure builds until failure of the seal and phreatic eruption occur.

Poás is not an isolated case where changes in gas chemistry precede phreatic eruptions. Rincón de la Vieja is a remote volcano in northern Costa Rica that also hosts a hyper-acid lake and produced seismically registered phreatic eruptions in September and October of 2014. Multi-GAS surveys were conducted in March of 2013 (Aiuppa et al., 2014), April of 2014, and October of 2014 and a six-fold increase in SO_2/CO_2 (Fig. 7) as well as a very large increase in SO_2/H_2S are observed in association with the transition from non-eruptive to eruptive behavior. Rare clear weather conditions on 14 April 2014 allowed us to measure SO_2 flux for the first time at Rincón de la Vieja (66 ± 17 T/d), which constrains the CO_2 flux to 312 ± 193 T/day. Although these most recent eruptions at Rincón de la Vieja were small, larger phreatic to phreato-magmatic

events (VEI 2–3) at this volcano have produced eruptive columns up to ∼4 km asl and generated destructive lahars.

Factors other than changes in gas flux and variations in the delivery of magmatic heat from depth must also play a role in the generation of phreatic eruptions and their size. The observation that the CO_2 flux at Rincón de la Vieja in April 2014 (before eruption) was an order of magnitude higher than at Poás during eruptive behavior (Fig. 5) suggests that differences in magmatic-hydrothermal plumbing systems dictate the heat flux threshold needed to generate phreatic eruptions, which probably plays a fundamental role in the potential for large phreatic explosions. Changes in the physical characteristics of the Poás lake are small (less than 10% volume change based on webcam images and field lake level measurements) compared to changes in gas fluxes (Fig. 6) and occur on longer timescales than the highly transient pulses of high temperature gas that generate individual phreatic blasts. Thus, changes in lake volume at Poás were probably not large enough to be the primary control on phreatic activity on short timescales. The composition of the gas emitted by the lake and the sulfur isotope systematics (Kusakabe et al., 2000; Rowe, 1994) indicate that the sublimnic hydrothermal systems are more influential on gas chemistry than superficial acid lakes. However, surficial physical changes may superimpose an additional control on the occurrence of phreatic eruptions. At the time of writing no phreatic eruptions had occurred at Poás since October of 2014. Since then the lake level has risen by ∼4 m and H_2S has appeared in lake gas emissions. An outstanding question at Poás is whether a decrease in heat flux led to both an increase in lake level and the cessation of eruptions, or whether increased meteoric water input increased the hydraulic pressure in the sublimnic hydrothermal system, which may have caused magmatic gases and heat to be channeled through the dome fumaroles, resulting in the cessation of phreatic eruptions. This topic is the subject of ongoing research.
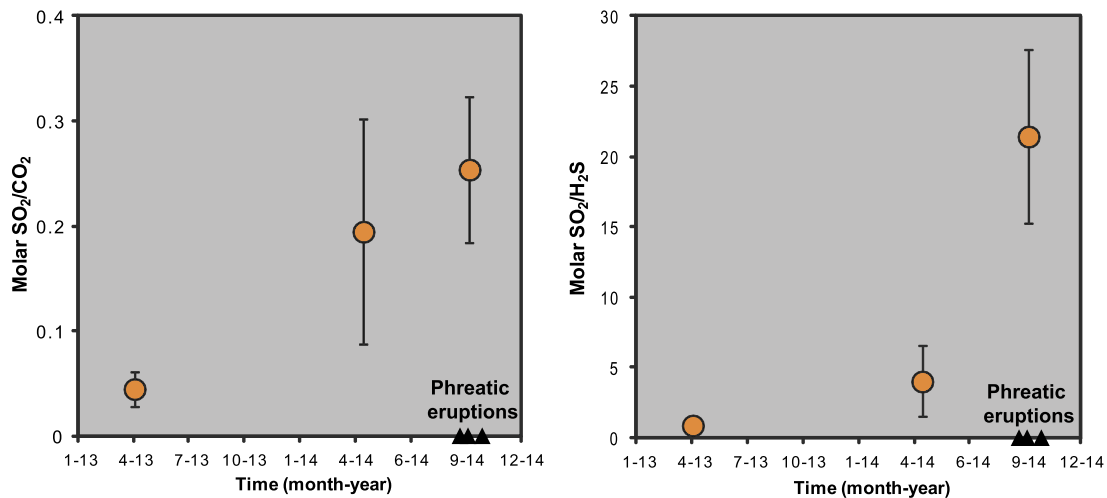
Fig. 7. Results of Multi-GAS campaigns conducted at Rincón de la Vieja volcano (Northern Costa Rica), which also hosts an ultra-acid crater lake. Data for April 2013 from Aiuppa et al. (2014). Seismically registered phreatic eruptions occurred in September and October of 2014 and were associated with significant increase in SO_2/CO_2 and SO_2/H_2S.

5. Conclusions

Phreatic eruptions occurring through crater lakes represent the wet endmember of a spectrum of "non-magmatic" eruption types (Rouwet et al., 2014a). Here, we show that high frequency gas monitoring may provide a vital short- to medium-term precursor heralding phreatic blasts and that these eruptions are the direct result of fluctuations in magmatic gas flux from depth. Sano et al. (2015) recently showed that the 2014 Mt. Ontake eruption was preceded by a long-term increase in $^3He/^4He$, which was similarly interpreted to represent increased supply of magmatic volatiles to the hydrothermal system. Together, these promising results call for enhanced gas monitoring at volcanoes prone to phreatic eruptions because magmatic heat, transferred by gases, is the driving force behind these eruptions. We show that the transition from non-eruptive to eruptive state can occur due to relatively small changes in gas input (a factor of two; Fig. 6), which may not be detectable with standard geophysical methods. Traditional geochemical monitoring of volcanic lake water compositions has in many cases shown long-term geochemical changes associated with increased magmatic volatile input, but monthly sampling campaigns and laboratory-based approaches will not provide key short-term phreatic precursors (Rouwet et al., 2014b). Furthermore, temporal changes in crater lake water chemistry are likely buffered by fluid residence time in the sublimnic hydrothermal system (Kusakabe et al., 2000). Gases, on the other hand, can pass rapidly through this reaction zone and dynamic changes in the sublimnic system determine the extent to which reactive species are stripped from the magmatic gas. Short-term precursors are the indicators needed in order to meaningfully forecast eruptions and to evacuate proximal areas. Real-time, high frequency, *in situ* gas monitoring may provide the missing link between long term signals of volcanic reactivation and sudden onset of phreatic eruption.

Explosive volcanic eruptions involving interaction with water are a diverse, poorly characterized, and particularly hazardous category of eruptions that remain the most challenging to forecast by traditional volcano monitoring techniques. Here we show that individual phreatic eruptions at Poás are preceded by changes in lake gas composition due to increasing input of magmatic volatiles. This finding suggests an intricate tie between shallow-sourced eruptions and short-period fluctuations in magma degassing intensity. These processes and associated precursory signals likely operate at many volcanoes where magmatic gases sustain hydrothermal systems prone to phreatic eruptions. Our results call for high frequency real-time monitoring of gas emissions at volcanoes to advance understanding of short-term changes in magma degassing, shallow energy storage, and associated volcanic hazards.

Appendix A. Supplementary material

Supplementary material related to this article can be found online at http://dx.doi.org/10.1016/j.epsl.2016.02.056.

References

Aiuppa, A., et al., 2007. Forecasting Etna eruptions by real-time observation of volcanic gas composition. Geology 35, 1115–1118.

Aiuppa, A., et al., 2009. The 2007 eruption of Stromboli volcano: insights from the real-time measurement of the volcanic gas plume CO_2/SO_2 ratio. J. Volcanol. Geotherm. Res. 182, 221–230.

Aiuppa, A., et al., 2013. First observations of the fumarolic gas output from a restless caldera: implications for the current period of unrest (2005–2013) at Campi Flegrei. Geochem. Geophys. Geosyst. 14, 4153–4169.

Aiuppa, A., et al., 2014. Gas measurements from the Costa Rica–Nicaragua volcanic segment suggest possible along-arc variations in volcanic gas chemistry. Earth Planet. Sci. Lett. 407, 134–147.

Barberi, F., Bertagnini, A., Landi, P., Principe, C., 1992. A review on phreatic eruptions and their precursors. J. Volcanol. Geotherm. Res. 52, 131–246.

Bennett, F., Raccichini, S., 1978. Subaqueous sulphur lake in Volcan Poas. Nature 271, 342–344.

Biggs, J., et al., 2014. Global link between deformation and volcanic eruption quantified by satellite imagery. Nature 5. http://dx.doi.org/10.1038/ncomms4471.

Brown, G., et al., 1989. Energy budget analysis for Poás crater lake: implications for predicting volcanic activity. Nature 339, 370–373.

Christenson, B.W., et al., 2007. Hazards from hydrothermally sealed volcanic conduits. Eos 88, 53–55.

Christenson, B.W., et al., 2010. Cyclic processes and factors leading to phreatic eruption events: insights from the 25 September eruption through Ruapehu Crater Lake, New Zealand. J. Volcanol. Geotherm. Res. 191, 15–32.

Delmelle, P., Bernard, A., Kusakabe, M., Fischer, T.P., Takano, B., 2000. Geochemistry of the magmatic-hydrothermal system of Kawah Ijen volcano, East Java, Indonesia. J. Volcanol. Geotherm. Res. 97, 31–53.

Fischer, T.P., et al., 2015. Temporal variations in fumarole gas chemistry at Poás volcano, Costa Rica. J. Volcanol. Geotherm. Res. 294, 56–70.

Galle, B., et al., 2002. A miniaturized ultraviolet spectrometer for remote sensing of SO_2 fluxes: a new tool for volcano surveillance. J. Volcanol. Geotherm. Res. 119, 241.

Giggenbach, W.F., et al., 1990. The chemistry of fumarolic vapor and thermal-spring discharges from the Nevado del Ruiz volcanic-magmatic-hydrothermal system, Colombia. J. Volcanol. Geotherm. Res. 42, 13–39.

Global Volcanism Program, 2013. Volcanoes of the World, v.4.4.1. Venzke, E. (Ed). Smithsonian Institution. Downloaded 15 Jan 2015. http://dx.doi.org/10.5479/si.GVP.VOTW4-2013.

Jolly, A.D., Sherburn, S., Jousset, P., Kilgour, G., 2010. Eruption source processes from seismic and acoustic observations of the 25 September 2007 Ruapehu – North Island, New Zealand. J. Volcanol. Geotherm. Res. 191, 35–43.

Kaneshima, S., et al., 1996. Mechanism of phreatic eruption at Aso volcano inferred from near-field broadband seismic observations. Science 273, 642–645.

Kusakabe, M., Komoda, Y., Takano, B., Abiko, T., 2000. Sulfur isotopic effects in the disproportionation reaction of sulfur dioxide in hydrothermal fluids: implications for the $\delta^{34}S$ variations of dissolved bisulfate and elemental sulfur from active crater lakes. J. Volcanol. Geotherm. Res. 97, 287–307.

Martínez, M., et al., 2000. Chemical evolution and volcanic activity of the active crater lake of Poás volcano, Costa Rica, 1993–1997. J. Volcanol. Geotherm. Res. 97, 127.

Mastin, L.G., Witter, J.B., 2000. The hazards of eruptions through lakes and seawater. J. Volcanol. Geotherm. Res. 97, 195–214.

Oppenheimer, C., Stevenson, D., 1989. Liquid sulphur lakes at Poás volcano. Nature 342, 790–793.

Pasternack, G.B., Varekamp, J.C., 1997. Volcanic lake systematic I. Physical constraints. Bull. Volcanol. 58, 528–538.

Pering, et al., 2014. High time resolution fluctuations in volcanic carbon dioxide degassing from Mount Etna. J. Volcanol. Geotherm. Res. 270, 115–121.

Rouwet, D., et al., 2014a. Recognizing and tracking volcanic hazards related to non-magmatic unrest: a review. J. Appl. Volcanol. 3, 17.

Rouwet, D., Tassi, F., Mora-Amador, R.A., Sandri, L., Chiarini, V., 2014b. Past, present and future of volcanic lake monitoring. J. Volcanol. Geotherm. Res. 272, 78–97.

Rowe, G.L., 1994. Oxygen, hydrogen, and sulfur isotope systematic of the crater lake system of Poás Volcano, Costa Rica. Geochem. J. 28, 263–287.

Rowe, G.L., et al., 1992. Fluid-volcano interaction in an active stratovolcano: the crater lake system of Poás volcano, Costa Rica. J. Geophys. Res. 49, 23–51.

Sano, Y., et al., 2015. Ten-year helium anomaly prior to the 2014 Mt Ontake eruption. Sci. Rep. 5, 13069. http://dx.doi.org/10.1038/srep13069.

Shinohara, H., Yoshikawa, S., Miyabuchi, Y., 2015. In: Rouwet, D., Christenson, B.W., Tassi, F., Vandemeulebrouck, J. (Eds.), Volcanic Lakes. Springer, Heidelberg, pp. 201–217.

Symonds, R.B., Gerlach, T.M., Reed, M.H., 2001. Magmatic gas scrubbing: implications for volcano monitoring. J. Volcanol. Geotherm. Res. 108, 303–341.

Tamburello, G., et al., 2015. Intense magmatic degassing through the lake of Copahue volcano, 2013–2014. J. Geophys. Res., Solid Earth 120. http://dx.doi.org/10.1002/2015JB012160.

Werner, C., et al., 2008. Variability of passive gas emissions, seismicity, and deformation during crater lake growth at White Island Volcano, New Zealand, 2002–2006. J. Geophys. Res. 113, B01204.

Williams, S.N., et al., 1986. Eruption of the Nevado del Ruiz Volcano, Colombia, on 13 November 1985: gas flux and fluid geochemistry. Science 233, 964–967.